Macromolecules

ARTICLE

pubs.acs.org/Macromolecules

Molecular Dynamics Studies of the Size and Internal Structure of the PAMAM Dendrimer Grafted with Arginine and Histidine

Hwankyu Lee,*[,†] Joon Sig Choi,[‡] and Ronald G. Larson[§]

[†]Department of Chemical Engineering, Dankook University, Yongin 448-701, South Korea

[‡]Department of Biochemistry, College of Natural Sciences, Chungnam National University, Daejeon 305-764, South Korea

[§]Department of Chemical Engineering, Biomedical Engineering, Mechanical Engineering, and Macromolecular Science and Engineering Program, University of Michigan, Ann Arbor, Michigan 48109, United States

ABSTRACT: G4 PAMAM dendrimers with each of the 64 termini grafted with zero to three histidine (His) residues followed by an end-grafted arginine (Arg) were simulated at two levels of protonation to mimic their electrostatic charges at pH 5 and 7. Arg is cationic at both pH values, and His is cationic only at pH 5. The simulations were carried out with a coarse-grained (CG) dendrimer force field that had previously predicted sizes and pH-dependent transitions between dense-core and dense-shell structures that were in agreement with experiments and all-atom simulations. In the work reported here, conjugation with Arg alone slightly increases the size of the dendrimer-conjugate complex at both pH 5 and 7 relative to that of the unmodified G4 dendrimer. Additional conjugation with His (pK_a of ~6.0), and with Arg again at the dendrimer terminals, does not change the complex size at pH 7 (at which His is neutral) relative to that with Arg alone, but at pH 5 (at which His is cationic), the addition of His does increase dendrimer size, showing that increased charge increases dendrimer swelling. The increased size may increase the cytotoxicity of the dendrimer at pH 5. Also, His conjugation induces a dense-core structure at pH 7 but does not change the dense-shell structure already present at pH 5 in the G4 dendrimer without amino acid conjugation. This indicates that the conjugation of His residues densifies the inner cavity of the dendrimer core at pH 7, leaving less room for other agents, and thus likely to lower drug encapsulation efficiency. These simulations suggest important possible effects of peptide conjugation on cytotoxicity and encapsulation efficiency at different pH, which need to be confirmed by experiments.

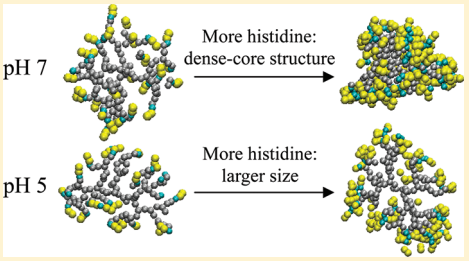

INTRODUCTION

Polyamidoamine (PAMAM) dendrimers are uniformly hyperbranched structures to which surface terminal groups can readily be added.[1,2] Because of their controlled mass, surface functionality, and good water solubility, they have great potential for biomedical applications such as drug delivery and antitumor therapeutics.[3−11] To improve their efficiency in these applications, dendrimers have been often modified, for example, by acetylating the cationic surface terminals to reduce cytotoxicity and nonspecific binding.[12−14] Also, conjugation with poly(ethylene glycol) (PEG) has been shown to reduce the cytotoxicity as well as increase the water solubility and circulating lifetime of dendrimers in the bloodstream because PEG chains sterically shield the dendrimer-encapsulated molecules.[15−17] To increase the specificity of targeting, ligands for certain receptors have been grafted to the dendrimer surface,[18] allowing the dendrimer-conjugate complexes to successfully target specific cancer cells in vitro and in vivo.[3,19]

Besides these methodologies, conjugation of peptides to the dendrimer surface also significantly improves transfection efficiency. Choi et al. found that the arginine-conjugated PAMAM dendrimers (PAMAM-Arg) show much higher gene-transfection efficiency than do the unmodified PAMAM dendrimers.[20] The increased charge of PAMAM-Arg only slightly increases cytotoxicity, leading to great potential of this component as a drug or gene carrier. Recently, different numbers of histidine (pK_a of 6.0), which is neutral at pH 7 and cationic at pH 5, were conjugated to PAMAM-Arg with Arg at the terminus, leading to even higher efficiency of the gene transfection into the cell nucleus than with PAMAM-Arg.[21] As a stage in the delivery to the cell nucleus, dendrimers are carried by the lysosome at pH ~5; thus, the effects of peptide conjugation on cytotoxicity and transfection efficiency at different pH values need to be understood. Since many experiments and simulations have shown that conformational and electrostatic properties of the dendrimer significantly modulate cytotoxicity and the efficiency of encapsulating drugs (or hydrophobic compounds),[22−24] the size and internal structure of the dendrimer−peptide complex should be examined as a function of pH. This information can be obtained more easily from simulations than from experiments. Many simulation studies have revealed the atomic-scale structure and dynamics of dendrimers and their interactions with polymers,[25−27] polyelectrolytes,[28−32] and lipid bilayers.[24,33−40] However, the conformational properties of the peptide-conjugated dendrimers and their

Received: August 24, 2011
Revised: September 26, 2011
Published: October 05, 2011

Table 1. List of Simulations

		no. of conjugates		no. of charges				
				dendrimer amines				
name	pH	histidine	arginine	tertiary (interior)	primary (surface)	histidine	arginine	total
G4-7	7				64			64
G4-R7	7		64				128	128
G4-HR7	7	64	64				128	128
G4-HHR7	7	128	64				128	128
G4-HHHR7	7	192	64				128	128
G4-5	5			62	64			126
G4-R5	5		64	62			128	190
G4-HR5	5	64	64	62		64	128	254
G4-HHR5	5	128	64	62		128	128	318
G4-HHHR5	5	192	64	62		192	128	382

interactions with lipid bilayers have not yet been studied through computation.

As a step toward understanding the effect of the peptide conjugation on cytotoxicity and the efficiency of encapsulation and transfection, we here report coarse-grained (CG) molecular dynamics (MD) simulations of dendrimers conjugated with varying numbers of histidine and arginine each at two levels of protonation, corresponding to the electrostatic charge on these residues at pH 5 and 7. The size and internal structure of the dendrimer-conjugate complex are examined by calculating radii, radial distribution functions, and densities of the dendrimer, water, and counterions. We find that the size and internal structure of the dendrimer depend on both conjugation level and pH, suggesting important effects of these parameters on dendrimer cytotoxicity and encapsulation efficiency.

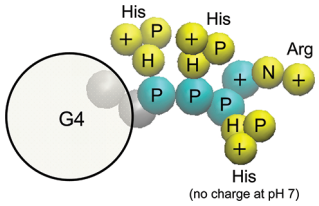

Figure 1. Coarse-grained model for the dendrimer-His-His-His-Arg (G4-HHHR5) complex at pH 5. Gray dots represent G4 dendrimer beads. Blue and yellow dots represent the amino acid backbones and side chains, respectively. "P", "*N*", "H", and "+" respectively designate polar, neutral, hydrophobic, and cationic beads. At pH 7, cationic beads of His are replaced with polar beads, leading to no charge for His. Note that the protonated N-terminal group of the backbone is represented by a cationic bead. The image was created with VMD.[49]

METHODS

All simulations and analyses were performed using the GROMACS4.5.3[41−43] simulation package with the "MARTINI" CG force field (FF) developed by Marrink et al.[44−46] The CG dendrimer FF has been previously optimized by our group to represent the experimentally measured and theoretically calculated size and internal structure of PAMAM dendrimers at different pH values.[26,37] In particular, this FF captured the transition from dense-core to dense-shell structure that occurs as pH is lowered, as observed in recent scattering experiments and all-atom simulations. For the peptide conjugates, we used the MARTINI amino-acid FF developed by Marrink et al.[46] This CG model lumps a few (3 or 4) heavy atoms into each CG bead. For example all three atoms (2 carbons and a nitrogen) of the backbone of each amino acid residue are lumped into a single bead, and the arginine and histidine side chains are represented by two and three beads, respectively. The MARTINI amino acid FF has been successfully used for protein−protein and protein−membrane interactions, although for each secondary structure, such as helix, extended (β-sheet), bend, turn, and unstructured (random coil), different sets of bond, angle, and dihedral potentials need to be imposed on the CG beads to describe the secondary structure of the protein. In this work, backbone beads were modeled using the potentials for random coils.

We linked all 64 surface-terminals of a G4 dendrimer to the amino acid conjugates, -Arg, -His-Arg, -His-His-Arg, and -His-His-His-Arg (Table 1). At pH 5, both the tertiary amines of the dendrimer interior and the primary amines of the dendrimer surface are protonated, while only the primary amines of the dendrimer surface are protonated at pH 7. When the dendrimer is conjugated with amino acids, its surface charges (primary amines) are removed. Figure 1 shows the schematic structure of the G4-HHHR complex at pH 5. The amino acid backbones are represented by polar beads except that N-terminal of Arg is modeled by a cationic bead because of its pK_a of ∼10. Side chains of amino acids are represented by polar, neutral, hydrophobic, and cationic beads, depending on the particular amino acid. Note that Arg is protonated at both pH 5 and 7, while His is protonated only at pH 5.

A single dendrimer-conjugate complex was solvated with ∼36 000 CG waters (representing ∼144 000 real waters, since in the CG model four waters are lumped into a single bead) in a periodic box of size 16.4 nm/side. Enough counterions were added to achieve electroneutrality. A temperature of 310 K and a pressure of 1 bar were maintained by applying a Berendsen thermostat in the NPT ensemble.[47] The LJ potential was smoothly shifted to zero between 9 and 12 Å. For the Coulomb potential, a cutoff of 12 Å was applied with long-range electrostatics using particle mesh Ewald summation (PME).[48] Simulations were performed for 1 μs with a time step of 20 fs, and the last 500 ns was used for analyses.

RESULTS AND DISCUSSION

We simulated G4 dendrimers with each terminus grafted with zero to three histidine residues and capped with a single arginine in water and counterions for 1 μs. Table 1 shows the numbers of conjugates and charges for all simulation systems at pH 5 and 7. In the names of the simulations, the first number "4" represents the dendrimer generation number, and the second number "5" or "7" indicates the pH value. The initials "H" and "R" respectively represent histidine and arginine conjugates. Thus, "G4-HHHR7" indicates that the conjugate -His-His-His-Arg is grafted onto the surface terminals of G4 dendrimers at pH 7. This study is basically based on the recent report by Yu et al.[21] in which it was demonstrated that the conjugation yield of the PAMAM G4 dendrimer with the respective peptides was more than 95% of the terminal amines.

Effect of the Peptide Conjugation on Dendrimer Size. The effect of the conjugated His and Arg residues on the radii of gyration (R_g) and outer radii (R) of the dendrimers and the dendrimer-conjugate complexes were calculated. The outer radii were taken to be the root-mean-squared (rms) distance from the terminal bead of the dendrimer (or Arg residue for the complex) to the center of mass (COM) of the dendrimer. For dendrimer-conjugate complexes, we also define the outer radius of the "dendrimer component" of the complex, where the "dendrimer component" includes only dendrimer beads (i.e., excludes the amino acid beads). The "outer radius" of the dendrimer component is the rms distance from the terminal bead of the dendrimer component to the COM of the dendrimer. Figure 2 shows that the R_g values of the dendrimer-conjugate complexes reach steady-state values at ~400 ns, indicating that simulations are equilibrated within the simulated time scale. Table 2 and Figure 3 show that dendrimer size increases with conjugation level at pH 5. The R_g and R values for G4-HHHR5 are higher by ~39% than those for G4-5, as expected, since this His-, Arg-conjugation increases the dendrimer charge, leading to dendrimer swelling, as observed in our previous work on the effect of dendrimer charge.[36,37] At pH 7, G4-R7 is larger than G4-7, similarly because of the dendrimer swelling induced by the increased number of charges, since Arg conjugation adds two charges per Arg (one on the side chain, and one remains on the backbone since the Arg backbone is a terminal amino acid), while removing only one terminal charge from the unconjugated G4. However, addition of

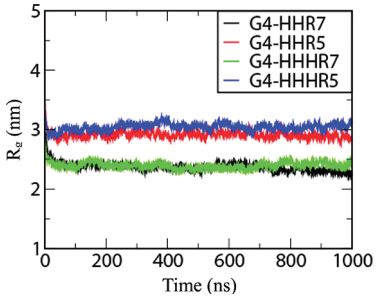

Figure 2. Radii of gyration (R_g) of G4-HHR and G4-HHHR complexes at pH 5 and 7 as a function of time.

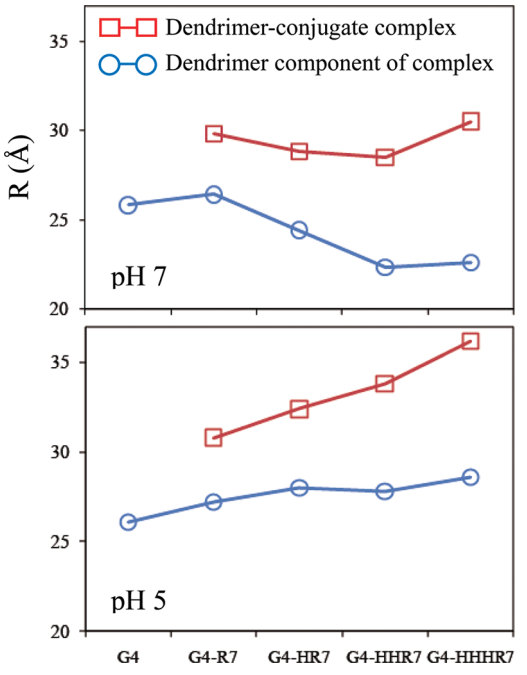

Figure 3. Average outer radii (R) of the dendrimer-conjugate complex and its dendrimer component at pH 7 (top) and pH 5 (bottom). Errors are within 0.2 Å.

Table 2. Radius of Gyration (R_g), Outer Radius (R), and Thickness of the Conjugate Layer of the Dendrimer and the Dendrimer-Conjugate Complex[a]

	R_g		R		
	dendrimer	complex	dendrimer	complex	thickness of conjugates
G4-7[b]	21.7 ± 0.1		25.8 ± 0.1		
G4-R7	22.0 ± 0.1	24.7 ± 0.1	26.4 ± 0.1	29.8 ± 0.1	3.4
G4-HR7	20.4 ± 0.1	24.1 ± 0.1	24.4 ± 0.1	28.8 ± 0.1	4.4
G4-HHR7	18.5 ± 0.1	23.0 ± 0.1	22.3 ± 0.1	28.5 ± 0.1	6.2
G4-HHHR7	18.9 ± 0.1	24.3 ± 0.1	22.6 ± 0.1	30.5 ± 0.1	7.9
G4-5[b]	21.9 ± 0.1		26.1 ± 0.1		
G4-R5	22.6 ± 0.1	25.7 ± 0.1	27.2 ± 0.1	30.8 ± 0.1	3.6
G4-HR5	23.2 ± 0.1	27.9 ± 0.1	28.0 ± 0.1	32.4 ± 0.1	4.4
G4-HHR5	22.9 ± 0.1	28.8 ± 0.1	27.8 ± 0.1	33.8 ± 0.1	6.0
G4-HHHR5	23.6 ± 0.1	30.6 ± 0.1	28.6 ± 0.1	36.2 ± 0.1	7.6

[a] All quantities are in Å. [b] Reference 26.

dx.doi.org/10.1021/ma2019396 |*Macromolecules* 2011, 44, 8681–8686

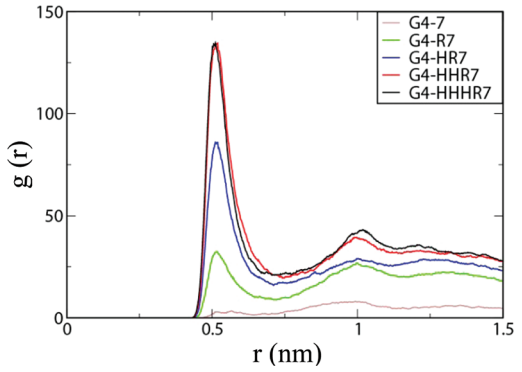

Figure 4. Radial distribution functions between the dendrimer-terminal beads at pH 7.

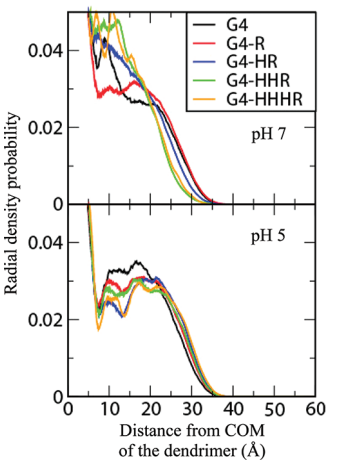

Figure 5. Radial density probabilities of the dendrimer component in the dendrimer-conjugate complex as a function of distance from center of mass (COM) of the dendrimer.

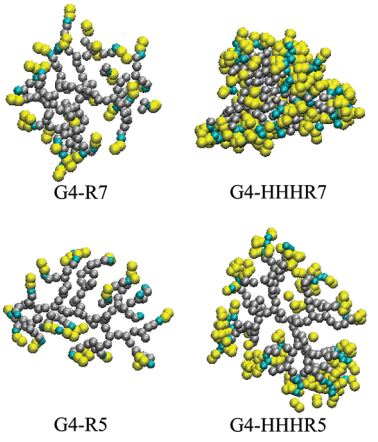

Figure 6. Snapshots of the cross section of the dendrimer-conjugate complex at the end (1 μs) of simulations. Blue, yellow, and gray dots represent the amino acid backbones, side chains, and dendrimer beads, respectively. The explicit water and ions are omitted for clarity.

His residues, which are neutral at pH 7, has almost no effect on size, as we see in Table 2 for G4-R7, G4-HR7, G4-HHR7, and G4-HHHR7. This is because increased conjugation of His residues increases the thickness of the conjugate layer on the dendrimer surface, but also slightly decreases the size of the underlying dendrimer component at pH 7, leading to an unchanged complex size overall (Figure 3). Here, the conjugate thickness is defined as the difference between the outer radius (R) of the dendrimer component and that of the whole dendrimer-conjugate complex.

To further examine this effect, radial distribution functions between the terminals of the dendrimer component were calculated. In Figure 4, G4-HHR7 and G4-HHHR7 show higher peaks than do others, indicating closer distances between dendrimer terminals, which are caused by the decreased swelling of the dendrimers with more His residues. These results indicate that the conjugation of a single Arg increases the particle size and surface-charge density at both pH 7 and 5, but the conjugation of His residues increases them only at pH 5. These results suggest that conjugation of His residues may modulate cytotoxicity and membrane permeability through dendrimer size effects at pH 5, but not at pH 7.

Effect of the Peptide Conjugation on Internal Structure. Although His conjugation does not affect the size of the dendrimer-conjugate complexes at pH 7, it does affect the size of their dendrimer components, as shown in Figure 3. This result implies that the internal structure of the dendrimer is affected by His conjugation. To investigate this, radial density profiles were calculated. Our previous work showed a dense-core structure (i.e., a maximum density at the dendrimer core) for G4, G5, and G7 at high pH and a dense-shell structure (i.e., a minimum density at the dendrimer core) at low pH, in agreement with recent scattering experiments and all-atom simulations.[26] Figure 5 (top) shows that the radial density profiles of the dendrimer component of G4-HR7, G4-HHR7, and G4-HHHR7 have higher peaks at the core (5−15 Å) than do G4-7 and G4-R7, indicating a dense-core structure for the former. This is consistent with our earlier observation that increased conjugation of His residues shrinks the dendrimer component at pH 7. At pH 5, the dense-shell structure shown in Figure 5 (bottom) is similar for all the above dendrimer complexes, indicating that the increased charges from the conjugated His at pH 5 do not change the internal structure of the dendrimer, which is already swollen due to the charges that are present inside the dendrimer at pH 5, so that addition of charged His to the dendrimer surface cannot swell the dendrimer core much further. At pH 7, addition of neutral His to the dendrimer surface removes the charge of the dendrimer surface and displaces the terminal charges of Arg farther from the dendrimer surface, which may reduce the swelling of the dendrimer component of the dendrimer-conjugate complex. In Figure 6, snapshots of the cross section of the dendrimer-conjugate complex show that G4-HHHR7 has a denser core structure than does G4-R7, while both G4-R5 and G4-HHHR5 have a dense-shell structure, consistent with observations in Figure 5.

Effect on the Encapsulation Efficiency and Cytotoxicity. Drugs or hydrophobic compounds can be encapsulated in the inner cavity of dendrimer cores and delivered to specific cells. To investigate the effect of peptide conjugation on encapsulation efficiency, the densities of water molecules were calculated as a function of distance from COM of the dendrimer component of the dendrimer-conjugate complex. In Figure 7, dendrimers with more His conjugates at pH 7 show lower densities of water, indicating a smaller inner vacancy in the dendrimer core and a dense-core structure, as observed in Figures 5 and 6. As the

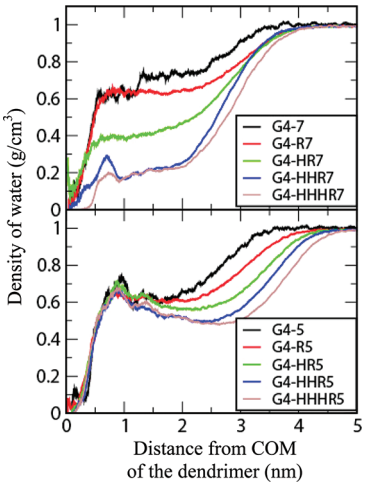

Figure 7. Density of water (g/cm^3) as a function of distance from COM of the dendrimer component in the dendrimer-conjugate complex.

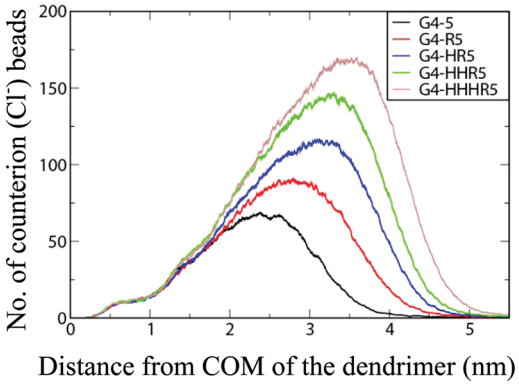

Figure 8. Number of counterion (Cl^-) beads as a function of the distance from COM of the dendrimer at pH 5.

distance from COM increases, the density values reach ~1 g/cm^3, confirming that the CG model correctly predicts the density of pure water. At pH 5, the conjugation of His residues does not influence the water density in the dendrimer core (0.5−1.5 nm from COM), indicating a relatively large inner vacancy and a dense-shell structure, as also observed in Figures 5 and 6. Heavier conjugation decreases water density at 2−4 nm from COM, presumably because of longer conjugates and more counterions. Figure 8 shows the number of counterions (Cl^-) as a function of the distance from the dendrimer COM. There are roughly equal numbers of ions at the core of each dendrimer, but more ions are found near the surface of the dendrimer with more conjugates. These results indicate that at pH 5 the conjugation of His residues increases the interaction of the dendrimer surface with counterions but does not change the internal structure of the dendrimer core. We note here that the CG model does not have partial charges on water. To compensate for the neglect of explicit polarization, screening of electrostatic interactions is done implicitly by assuming a uniform relative dielectric constant (ε = 15), which compromises between the large ε in water and small ε in the hydrophobic regions. Because of the implicit screening, the interaction strength of polar substances is underestimated in nonpolarizable solvents, such as that used in our simulations. Thus, our predicted ion distribution should be view with caution.

Experimentally, the Arg-conjugated G4 dendrimer has shown much higher transfection efficiency than does the unmodified dendrimer.[20] Also, although the surface-charge density for the Arg-conjugated dendrimer is twice as high as for the unmodified dendrimers, experiments show that the unmodified G4 dendrimer and the G4 dendrimer conjugated with -Arg, -His-Arg, -His-His-Arg, or -His-His-His-Arg show almost the same cytotoxicity at pH 7.[21] Our simulation results show that conjugation by His does not change the particle size at pH 7, at which His is neutral. Since the charge density and particle size are important factors for cytotoxicity,[23,24,38] this suggests that His conjugation may not affect cytotoxicity at pH 7, which is consistent with experiments.[21] However, at pH 5, cationic His residues swell the dendrimer significantly, suggesting that increased surface charge and particle size may increase cytotoxicity at pH 5. Conjugation of His residues induces a dense-core structure at pH 7 but does not change the dense-shell structure of the unmodified dendrimer at pH 5, indicating that at pH 7 conjugation may reduce the vacancy in the dendrimer interior and lower encapsulation efficiency.

Experimental work should be performed to check these findings and their implications for the effect of peptide conjugation on cytotoxicity and encapsulation efficiency as a function of pH. Also, simulation studies of the interactions between peptide-conjugated dendrimers and membranes ought to be performed, which we hope to report on elsewhere.

CONCLUSIONS

G4 PAMAM dendrimers conjugated with different numbers of His and Arg residues were simulated at pH 5 and 7, mimicked by different levels of protonation, and using a version of the MARTINI coarse-grain (CG) force field (FF). This CG dendrimer FF had already been shown to predict the size and structural transitions between dense-core and dense-shell structures of G4, G5, and G7 PAMAM dendrimers at different pH values, in good agreement with recent scattering experiments and all-atom simulations. Using this FF, simulations show that the Arg-grafted dendrimer is slightly larger than the unmodified dendrimer. The increased particle size and net charges of the Arg-grafted dendrimer may slightly increase cytotoxicity, as observed in experiment. As more His residues are conjugated to the Arg-grafted dendrimer, the net charges and particle size significantly increase at pH 5, but not at pH 7 where His is neutral, suggesting that the increased surface charges and larger size may increase cytotoxicity of the dendrimer at pH 5. Also, increased conjugation with His residues induces a dense-core structure at pH 7 but does not change the dense-shell structure of the unmodified dendrimer at pH 5. These results indicate that increased His conjugation may result in a reduced free volume within the dendrimer core at pH 7, and this could reduce encapsulation efficiency. These findings regarding the size and internal structure of the peptide-conjugated dendrimer, which possibly modulate cytotoxicity and efficiency of transfection and encapsulation, motivate further systematic experimental studies.

AUTHOR INFORMATION

Corresponding Author

*E-mail: leeh@dankook.ac.kr.

ACKNOWLEDGMENT

The present research was conducted by the research fund of Dankook University in 2011. The authors acknowledge the

support from KISTI supercomputing center through the strategic support program for the supercomputing application research (No. KSC-2011-C2-12).

REFERENCES

(1) Naylor, A. M.; Goddard, W. A.; Kiefer, G. E.; Tomalia, D. A. *J. Am. Chem. Soc.* **1989**, *111*, 2339–2341.
(2) Tomalia, D. A.; Naylor, A. M.; Goddard, W. A. *Angew. Chem., Int. Ed. Engl.* **1990**, *29*, 138–175.
(3) Menjoge, A. R.; Kannan, R. M.; Tomalia, D. A. *Drug Discovery Today* **2010**, *15*, 171–185.
(4) Prosa, T. J.; Bauer, B. J.; Amis, E. J.; Tomalia, D. A.; Scherrenberg, R. *J. Polym. Sci., Part B: Polym. Phys.* **1997**, *35*, 2913–2924.
(5) Tomalia, D. A.; Reyna, L. A.; Svenson, S.; Portland Press Ltd.: 2007; pp 61−67.
(6) Patri, A. K.; Kukowska-Latallo, J. F.; Baker, J. R. *Adv. Drug Delivery Rev.* **2005**, *57*, 2203–2214.
(7) Choi, Y.; Thomas, T.; Kotlyar, A.; Islam, M. T.; Baker, J. R. *Chem. Biol.* **2005**, *12*, 35–43.
(8) Choi, Y. S.; Mecke, A.; Orr, B. G.; Holl, M. M. B.; Baker, J. R. *Nano Lett.* **2004**, *4*, 391–397.
(9) Majoros, I. J.; Williams, C. R.; Baker, J. R. *Curr. Top. Med. Chem.* **2008**, *8*, 1165–1179.
(10) Astruc, D.; Boisselier, E.; Ornelas, C. *Chem. Rev.* **2010**, *110*, 1857–1959.
(11) Patri, A. K.; Majoros, I. J.; Baker, J. R. *Curr. Opin. Chem. Biol.* **2002**, *6*, 466–471.
(12) Majoros, I. J.; Keszler, B.; Woehler, S.; Bull, T.; Baker, J. R. *Macromolecules* **2003**, *36*, 5526–5529.
(13) Hong, S. P.; Bielinska, A. U.; Mecke, A.; Keszler, B.; Beals, J. L.; Shi, X. Y.; Balogh, L.; Orr, B. G.; Baker, J. R.; Holl, M. M. B. *Bioconjugate Chem.* **2004**, *15*, 774–782.
(14) Hong, S. P.; Leroueil, P. R.; Janus, E. K.; Peters, J. L.; Kober, M. M.; Islam, M. T.; Orr, B. G.; Baker, J. R.; Holl, M. M. B. *Bioconjugate Chem.* **2006**, *17*, 728–734.
(15) Kim, Y.; Klutz, A. M.; Jacobson, K. A. *Bioconjugate Chem.* **2008**, *19*, 1660–1672.
(16) Luo, D.; Haverstick, K.; Belcheva, N.; Han, E.; Saltzman, W. M. *Macromolecules* **2002**, *35*, 3456–3462.
(17) Kojima, C.; Toi, Y.; Harada, A.; Kono, K. *Bioconjugate Chem.* **2007**, *18*, 663–670.
(18) Shukla, R.; Thomas, T. P.; Peters, J.; Kotlyar, A.; Myc, A.; Baker, J. R., Jr. *Chem. Commun.* **2005**, 5739–5741.
(19) Malik, N.; Evagorou, E. G.; Duncan, R. *Anti-Cancer Drugs* **1999**, *10*, 767–776.
(20) Choi, J. S.; Nam, K.; Park, J. Y.; Kim, J. B.; Lee, J. K.; Park, J. S. *J. Controlled Release* **2004**, *99*, 445–456.
(21) Yu, G. S.; Bae, Y. M.; Choi, H.; Kong, B.; Choi, I. S.; Choi, J. S. *Bioconjugate Chem.* **2011**, *22*, 1046–1055.
(22) Leroueil, P. R.; Berry, S. A.; Duthie, K.; Han, G.; Rotello, V. M.; McNerny, D. Q.; Baker, J. R.; Orr, B. G.; Holl, M. M. B. *Nano Lett.* **2008**, *8*, 420–424.
(23) Leroueil, P. R.; Hong, S. Y.; Mecke, A.; Baker, J. R.; Orr, B. G.; Holl, M. M. B. *Acc. Chem. Res.* **2007**, *40*, 335–342.
(24) Lee, H.; Larson, R. G. *J. Phys. Chem. B* **2008**, *112*, 7778–7784.
(25) Lee, H.; Larson, R. G. *J. Phys. Chem. B* **2009**, *113*, 13202–13207.
(26) Lee, H.; Larson, R. G. *Macromolecules* **2011**, *44*, 2291–2298.
(27) Lee, H.; Larson, R. G. *J. Phys. Chem. C* **2011**, *115*, 5316–5322.
(28) Lyulin, S. V.; Darinskii, A. A.; Lyulin, A. V. *Macromolecules* **2005**, *38*, 3990–3998.
(29) Lyulin, S. V.; Darinskii, A. A.; Lyulin, A. V. *Phys. Rev. E* **2008**, *78*, 9.
(30) Lyulin, S. V.; Vattulainen, I.; Gurtovenko, A. A. *Macromolecules* **2008**, *41*, 4961–4968.
(31) Maiti, P. K.; Bagchi, B. *Nano Lett.* **2006**, *6*, 2478–2485.
(32) Welch, P.; Muthukumar, M. *Macromolecules* **2000**, *33*, 6159–6167.
(33) Kelly, C. V.; Leroueil, P. R.; Nett, E. K.; Wereszczynski, J. M.; Baker, J. R.; Orr, B. G.; Holl, M. M. B.; Andricioaei, I. *J. Phys. Chem. B* **2008**, *112*, 9337–9345.
(34) Kelly, C. V.; Leroueil, P. R.; Orr, B. G.; Holl, M. M. B.; Andricioaei, I. *J. Phys. Chem. B* **2008**, *112*, 9346–9353.
(35) Kelly, C. V.; Liroff, M. G.; Triplett, L. D.; Leroueil, P. R.; Mullen, D. G.; Wallace, J. M.; Meshinchi, S.; Baker, J. R.; Orr, B. G.; Holl, M. M. B. *ACS Nano* **2009**, *3*, 1886–1896.
(36) Lee, H.; Baker, J. R.; Larson, R. G. *J. Phys. Chem. B* **2006**, *110*, 4014–4019.
(37) Lee, H.; Larson, R. G. *J. Phys. Chem. B* **2006**, *110*, 18204–18211.
(38) Lee, H.; Larson, R. G. *J. Phys. Chem. B* **2008**, *112*, 12279–12285.
(39) Lee, H.; Larson, R. G. *Molecules* **2009**, *14*, 423–438.
(40) Ginzburg, V. V.; Balijepailli, S. *Nano Lett.* **2007**, *7*, 3716–3722.
(41) Hess, B.; Kutzner, C.; van der Spoel, D.; Lindahl, E. *J. Chem. Theory Comput.* **2008**, *4*, 435–447.
(42) Lindahl, E.; Hess, B.; van der Spoel, D. *J. Mol. Model.* **2001**, *7*, 306–317.
(43) Van Der Spoel, D.; Lindahl, E.; Hess, B.; Groenhof, G.; Mark, A. E.; Berendsen, H. J. C. *J. Comput. Chem.* **2005**, *26*, 1701–1718.
(44) Marrink, S. J.; de Vries, A. H.; Mark, A. E. *J. Phys. Chem. B* **2004**, *108*, 750–760.
(45) Marrink, S. J.; Risselada, H. J.; Yefimov, S.; Tieleman, D. P.; de Vries, A. H. *J. Phys. Chem. B* **2007**, *111*, 7812–7824.
(46) Monticelli, L.; Kandasamy, S. K.; Periole, X.; Larson, R. G.; Tieleman, D. P.; Marrink, S. J. *J. Chem. Theory Comput.* **2008**, *4*, 819–834.
(47) Berendsen, H. J. C.; Postma, J. P. M.; van Gunsteren, W. F.; DiNola, A.; Haak, J. R. *J. Chem. Phys.* **1984**, *81*, 3684–3690.
(48) Essmann, U.; Perera, L.; Berkowitz, M. L.; Darden, T.; Lee, H.; Pedersen, L. G. *J. Chem. Phys.* **1995**, *103*, 8577–8593.
(49) Humphrey, W.; Dalke, A.; Schulten, K. *J. Mol. Graphics* **1996**, *14*, 33–38.